Institut für Numerische Simulation
Rheinische Friedrich-Wilhelms-Universität Bonn

Wegelerstraße 6 • 53115 Bonn • Germany
phone +49 228 73-3427 • fax +49 228 73-7527
www.ins.uni-bonn.de

S. Beuchler

Inexact additive Schwarz solvers for hp-FEM discretizations in three dimensions

INS Preprint No. 1107

July 2011

Inexact additive Schwarz solvers for hp-FEM discretizations in three dimensions

Sven Beuchler

Abstract In this paper, a boundary value problem of second order in three space dimensions is discretized by means of the hp-version of the finite element method. The system of linear algebraic equations is solved by the preconditioned conjugate gradient method with an overlapping domain decomposition preconditioner with inexact subproblem solvers. In addition to a global solver for the low order functions, the ingredients of this preconditioner are local solvers for the patches. Here, a solver is used which utilizes the tensor product structure of the patches. The efficiency in time and iteration numbers of the presented solver is shown in several numerical examples for diffusion like problems as well as for problems in linear elasticity.

1 Introduction

The numerical solution of boundary value problems (bvp) of partial differential equations (pde) is one of the major challenges in Computational Mathematics. Finite element methods (fem) are among to the most powerful tools in order to compute an approximate solution of bvp. For the h-version of the fem, the polynomial degree p of the shape functions on the elements is kept constant and the mesh-size h is decreased. This is in contrast to the p-version of the fem in which the polynomial degree p is increased and the mesh-size h is kept constant. Both ideas, mesh refinement and increasing the polynomial degree, can be combined. This is called the hp-version of the fem. The advantage of the p-version in comparison to the h-version is that the solution converges much faster to the exact solution with respect to the dimension N of the approximation space, see e.g. [30], [31], [13] and the references therein as well as [20] for the related spectral element methods.

Sven Beuchler
Institute for Numerical Simulation, Wegelerstraße 6, 53115 Bonn, Germany, e-mail: beuchler@ins.uni-bonn.de

From the literature it is known, see e.g. [32], that preconditioned conjugate gradient (pcg) methods with additive Schwarz preconditioners (asm) as domain decomposition (dd) are a powerful tool for the development of fast and efficient solvers for the h-version as well as for the p-version of the FEM. One class are nonoverlapping dd preconditioners with inexact subproblem solvers on the subdomains, [17]. This preconditioner requires a solver related to the Dirichlet problem on the elements $\triangle_s$, see [22, 4, 8, 14], a solver related to the Schur complement corresponding to the subdomain boundaries, see [19, 1], and an approximate discrete harmonic extension from $\partial\triangle_s$ to $\triangle_s$, see [3, 24, 5, 12, 16]. This leads to quasioptimal solvers for hp-fem discretizations in two space dimensions since the coupling between the high order basis functions and the low order basis functions can be removed by paying a $\log p$ term in the condition number estimates, [3].

In the three-dimensional case, the usage of nonoverlapping asm preconditioners is much more difficult due to the coupling between the different types of basis functions, see e.g. [23, 15, 26, 27] and the references therein. Another approach is using overlapping preconditioners as developed in [25], see also [29] for the tetrahedral case. This decouples the low order basis functions from the high order basis functions used in p-FEM. It remains the solution of high-order systems on patches consisting of about 8 hexahedrons. In [6], fast solvers for the patch structure are proposed. They incorporate the tensor product structure of the patches and are an extension of the results presented in [8]. Condition number estimates on the patches and the construction principle are also presented in [6]. We also refer to the recent publications [21, 11, 2].

The purpose of this paper is the presentation of the performance of the overlapping dd preconditioner [25] combined with the patch preconditioner of [6] as subproblem solver. Our first numerical experiments of this dd preconditioner for the p-version of the fem are presented for scalar elliptic problems as well as for the system of Lamé equations. In addition, the final condition number estimates are given in the theoretical part of the paper.

The outline of this paper is as follows. Section 2 describes the setting of the problem and the discretization. The definition of the preconditioners and the condition number estimates are presented in section 3. The main part of this paper is devoted to section 4. Several numerical experiments show the efficiency of the proposed solvers. Section 5 concludes the paper with possible generalizations of the presented results.

Throughout this paper, the integer p denotes the polynomial degree. For two real symmetric and positive definite $n \times n$ matrices A, B, the relation $A \preceq B$ means that $A - cB$ is negative definite, where $c > 0$ is a constant independent of n, or p. The relation $A \sim B$ means $A \preceq B$ and $B \preceq A$, i.e. the matrices A and B are spectrally equivalent. The isomorphism between a function $u = \sum_i u_i \psi_i \in L^2$ and the vector of coefficients $\underline{u} = [u_i]_i$ with respect to the basis $[\Psi] = [\psi_1, \psi_2, \ldots]$ is denoted as $u = [\Psi]\underline{u}$.

2 Setting of the problem, discretization

In this paper, we consider the following boundary value problem. Let $\Omega \subset \mathbb{R}^3$ be a bounded Lipschitz domain and $\mathbb{V}$ be a Sobolev space on Ω. Moreover, let $a : \mathbb{V} \times \mathbb{V} \mapsto \mathbb{R}$ be a $\mathbb{V}$ elliptic and bounded bilinear form and $F : \mathbb{V} \mapsto \mathbb{R}$ be a bounded linear functional. Then, we are looking for solutions of

$$\text{Find } u \in \mathbb{V} \quad \text{ such that } \quad a(u,v) = F(v) \quad \forall v \in \mathbb{V}. \tag{1}$$

Throughout this paper, the following types of bvp are investigated:

- Scalar elliptic problems of second order: Here, the corresponding Sobolev space is defined as $\mathbb{V} = H^1_{\Gamma_1}(\Omega) := \{u \in H^1(\Omega), u\,|_{\Gamma_1} = 0\}$ with $\Gamma_1 \subset \partial\Omega$ and $meas(\Gamma_1) > 0$. The bilinear form and the right hand side are given as

$$\begin{aligned} a(u,v) &= \int_\Omega \left(\nabla u(x) \cdot D(x) \nabla v(x) + c(x) u(x) v(x)\right)\, \mathrm{d}x, \\ F(v) &= \int_\Omega f(x) v(x)\, \mathrm{d}x + \int_{\partial\Omega\setminus\Gamma_1} \frac{\partial v}{\partial \mathfrak{n}}(x) f_1(x)\, \mathrm{d}S, \end{aligned} \tag{2}$$

  respectively. The functions $D : \overline{\Omega} \mapsto \mathbb{R}^+$ and $c : \overline{\Omega} \mapsto \mathbb{R}^+_0$ are assumed to be bounded and piecewise constant whereas $f \in L^2(\Omega)$, $f_1 \in L^2(\partial\Omega)$ and $\mathfrak{n}$ is the outer normal vector.
- The system of Lamé equations of linear elasticity: The Sobolev space is defined as $\mathbb{V} = (H^1_{\Gamma_1}(\Omega))^3$ with $meas(\Gamma_1) > 0$. The bilinear form and the right hand side are given as

$$\begin{aligned} a(u,v) &= \int_\Omega \frac{E}{2+2\nu}\left(\nabla u(x) : \nabla v(x) + \frac{1}{1-2\nu} \nabla \cdot u(x)\ \nabla \cdot v(x)\right)\, \mathrm{d}x, \\ F(v) &= \int_\Omega f(x) \cdot v(x)\, \mathrm{d}x + \int_{\partial\Omega\setminus\Gamma_1} \frac{\partial v}{\partial \mathfrak{n}}(x) \cdot f_1(x)\, \mathrm{d}S, \end{aligned} \tag{3}$$

  respectively. The functions $E : \overline{\Omega} \mapsto \mathbb{R}^+$ and $\nu : \overline{\Omega} \mapsto (0, \frac{1}{2})$ are assumed to be bounded and piecewise constant whereas $f \in (L^2(\Omega))^3$ and $f_1 \in (L^2(\partial\Omega))^3$.

Problem (1) is discretized by means of the *hp*-version of the finite element method using hexahedral elements $\triangle_s$, $s = 1, \ldots, nel$. Let $\hat{\triangle} = (-1,1)^3$ be the reference hexahedron and $F_s : \hat{\triangle} \to \triangle_s$ be the isoparametric mapping to the element $\triangle_s$. We define the space $\mathbb{M}_p := \left(\{u \in H^1_{\Gamma_1}(\Omega), u\,|_{\triangle_s} = \tilde{u}(F_s^{-1}(x,y,z)), \tilde{u} \in \mathbb{Q}_p\}\right)^d$ with $d = 1$ or $d = 3$, where $\mathbb{Q}_p$ is the space of all polynomials of maximal degree p in each variable. In order to obtain a basis for $\mathbb{M}_p$, let

$$\hat{L}_i(x) = \frac{1}{2}(2i-1)\int_{-1}^{x} L_{i-1}(s)\,\mathrm{d}s, \quad i = 1,\dots,p, \quad \hat{L}_0(x) = \frac{1-x}{2} \tag{4}$$

be the i-th integrated Legendre polynomial where $L_i(x) = \frac{1}{2^i i!}\frac{\mathrm{d}^i}{\mathrm{d}x^i}(x^2-1)^i$ denotes the i-th Legendre polynomial. On the reference element $\hat{\triangle} = (-1,1)^3$, the local basis functions

$$\hat{L}_{ijk}(x,y,z) = \hat{L}_i(x)\hat{L}_j(y)\hat{L}_k(z), \quad i,j,k = 0,\dots,p \tag{5}$$

are used. Since $\hat{L}_i(\pm 1) = 0$, $i \geq 2$, the global basis $[\mathtt{H}] = (\zeta_1,\dots,\zeta_N)$ for $\mathbb{M}_p$ is built in the usual way, by using the vertex functions (V), the edge bubble functions (E), face bubble functions (F), and the interior bubble functions (I), locally on each element $\triangle_s$, and globally on Ω. We refer the interested reader to [13] and the references therein concerning the details.

The Galerkin projection of (1) onto the N-dimensional space $\mathbb{M}_p$ leads to the linear system of algebraic finite element equations

$$\mathscr{K}_\zeta \underline{u} = \underline{f}, \quad \text{where} \quad \mathscr{K}_\zeta = [a(\zeta_j,\zeta_i)]_{i,j=1}^N, \quad \underline{f} = [F(\zeta_i)]_{i=1}^N. \tag{6}$$

Using the vector $\underline{u}$, an approximation $u_p = [\mathtt{H}]\underline{u}$ of the exact solution u of (1) is obtained by the usual finite element isomorphism.

3 The solution of the linear system

This section is devoted to the solution of the system of linear algebraic equations (6). It is distinguished between discretizations of scalar elliptic equations as in (2) and the system of Lamé equations as in (3).

3.1 The scalar elliptic case

In this subsection, we consider the bilinear form $a(\cdot,\cdot)$ (2) which is elliptic and bounded on the Sobolev space $\mathbb{V} = H^1_{\Gamma_1}(\Omega)$. It is intended to use an overlapping dd preconditioner which has been developed by Pavarino, [25]. For the definition of the preconditioner, some notation is introduced. Let

$$\mathbb{U}_0 = \left\{u \in H^1_{\Gamma_1}(\Omega), u\,|_{\triangle_s} = \tilde{u}(F_s^{-1}(x,y,z)), \tilde{u} \in \mathbb{Q}_1\right\} \tag{7}$$

be the space of all finite element functions of maximal polynomial degree 1. For a given node $\mathtt{v}$, let $\Omega_\mathtt{v} = \{\cup_s \overline{\triangle_s}, \mathtt{v} \subset \overline{\triangle_s}\}$ be the closed patch associated to a node $\mathtt{v}$ of the finite element mesh. Then, for each node $\mathtt{v}$ of the finite element mesh, we introduce

$$\mathbb{U}_{\mathrm{v}} = \left\{ u \in \mathbb{M}_p, \operatorname{supp} u \subset \Omega_{\mathrm{v}} \right\} \tag{8}$$

as the patch space, cf. an analogous two-dimensional example in Figure 1.

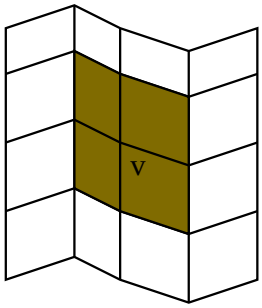

Fig. 1 Patch Ω_{v} of a node v (2D) (marked colored).

Theorem 3.1 *Let $\mathbb{U}_v$ and $\mathbb{U}_0$ be defined via* (8) *and* (7)*, respectively. Then, for all $u \in \mathbb{M}_p$ there exists a decomposition $u = u_0 + \sum_{\mathrm{v}} u_{\mathrm{v}}, u_0 \in \mathbb{U}_0, u_{\mathrm{v}} \in \mathbb{U}_{\mathrm{v}}$ such that*

$$a(u,u) \succeq b(u,u) := \inf_{u=u_0+u_{\mathrm{v}}} \left(a(u_0,u_0) + \sum_{\mathrm{v}} a(u_{\mathrm{v}},u_{\mathrm{v}}) \right).$$

Moreover, for all decompositions $u = u_0 + \sum_{\mathrm{v}} u_{\mathrm{v}}, u_0 \in \mathbb{U}_0, u_{\mathrm{v}} \in \mathbb{U}_{\mathrm{v}}$

$$a(u,u) \preceq a(u_0,u_0) + \sum_{\mathrm{v}} a(u_{\mathrm{v}},u_{\mathrm{v}}).$$

The constants depend neither on h nor p.

Proof. This result has been proven by Pavarino [25].

Remark 3.2 *The bilinear form $b(\cdot,\cdot)$ in Theorem 3.1 defines a preconditioner C_ζ for $\mathscr{K}_\zeta$* (6) *in the following way. Let $J(\mathrm{v}) = \left[j_1^{\mathrm{v}}, \ldots, j_{n_{\mathrm{v}}}^{\mathrm{v}} \right]$ be the index set of all basis functions ζ_j with $\operatorname{supp}(\zeta_j) \subset \Omega_{\mathrm{v}}$ and $J(0)$ the index set of all vertex functions (V). Due to the partition of* [H] *into vertex, edge, face and interior functions, the set $[\zeta_j]_{j \in J(\mathrm{v})}$ forms a n_{v} dimensional basis of the space $\mathbb{U}_{\mathrm{v}}$. Let $P_{\mathrm{v}} \in \mathbb{R}^{n_{\mathrm{v}} \times N}$ be the Boolean matrix with the entries*

$$[P_{\mathrm{v}}]_{ij} = \begin{cases} 1 \text{ if } j = j_i^{\mathrm{v}}, 1 \le i \le n_{\mathrm{v}} \\ 0 \qquad\qquad \text{else} \end{cases}.$$

Finally, let

$$C_{\mathrm{v}} = \left[a(\zeta_{j_i^{\mathrm{v}}}, \zeta_{j_k^{\mathrm{v}}}) \right]_{i,k=1}^{n_{\mathrm{v}}}. \tag{9}$$

In the same way, P_0 and C_0 corresponding to the set $J(0)$ are introduced. Then, the splitting in Theorem 3.1 introduces the preconditioner

$$C_\zeta^{-1} = P_0^\top C_0^{-1} P_0 + \sum_{\mathrm{v}} P_{\mathrm{v}}^\top C_{\mathrm{v}}^{-1} P_{\mathrm{v}} \tag{10}$$

with $\mathscr{K}_\zeta \sim C_\zeta$, see e.g. [32].

Therefore, in the sense of inexact asm it suffices to develop preconditioners for C_0 and C_{v} where v is running over all non Dirichlet nodes v of the mesh. The system for C_0 corresponds to all low order basis functions. Here, many solvers in the sense of inexact additive Schwarz preconditioners are available for a solution in optimal arithmetical complexity. Examples are multigrid methods, [18], and PCG-methods with the BPX-preconditioner, [10], for structured meshes and algebraic multigrid methods (AMG), [28], for unstructured meshes. For the construction of the preconditioner for C_{v} (9), let us make the following mesh

Assumption 3.3 *Each patch Ω_{v} corresponding to an interior node is the union of eight hexahedrons, two in each space direction. Patches to Neumann nodes on faces of Ω are assumed to be the union of four hexahedrons.*

For interior nodes, the patch Ω_{v} is transformed to the reference patch $\hat{\Omega} = [-2,2]^3$ consisting of eight cubes of length 2. Let $\mathbb{U}_{\mathrm{v}}$ be defined as in (8). This space is equipped with the basis of the integrated Legendre polynomials of (5) denoted as $[\Phi_3] = [\phi_{I,3}]_{I=1}^M$, $M = (2p-1)^3$. Using the lexicographic ordering for the local functions, (5) and the structure of $\hat{\Omega}$, the basis functions can be expressed as products of one-dimensional basis functions, e.g.

$$\begin{aligned} \phi_{I,3}(x,y,z) = \phi_{i,1}(x)\phi_{j,1}(y)\phi_{k,1}(z), \quad 1 \le i,j,k \le 2p-1 \\ I = (2p-1)^2(k-1) + (2p-1)(j-1) + i \end{aligned} \tag{11}$$

with the one-dimensional functions $[\Phi_1] := [\phi_{i,1}]_{i=1}^{2p-1}$. These one-dimensional functions are shifted integrated Legendre polynomials (4). More precisely,

$$\begin{aligned} \phi_{1,1}(x) &= \frac{1}{2}\begin{cases} 2+x & x \in [-2,0] \\ 2-x & x \in [0,2] \\ 0 & \text{else} \end{cases}, \\ \phi_{i,1}(x+1) &= \begin{cases} \hat{L}_i(x) & |x| \le 1 \\ 0 & \text{else} \end{cases}, \ i = 2,\dots,p, \\ \phi_{p+i-1,1}(x-1) &= \begin{cases} (-1)^i \hat{L}_i(x) & |x| \le 1 \\ 0 & \text{else} \end{cases}, \ i = 2,\dots,p. \end{aligned} \tag{12}$$

The basis functions (12) for $p = 3$ are displayed in Figure 2. The finite element isomorphism introduces the matrix $\hat{K}_{3,p}$ by the relation

$$a(u_p, v_p) = \underline{u}^\top \hat{K}_{3,p} \underline{v} \quad \forall u_p = [\Phi_3]\underline{u}, v_p = [\Phi_3]\underline{v}. \tag{13}$$

For the bilinear form of the Laplacian $a(u,v) = \int_{\hat{\Omega}} \nabla u \cdot \nabla v$, equations (11) and (13) imply

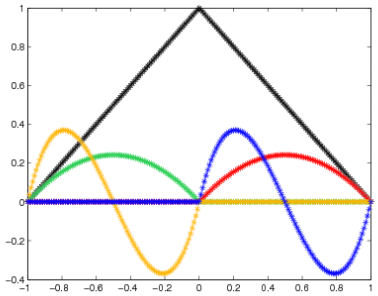

Fig. 2 One dimensional basis functions on the patch for $p = 3$.

$$\hat{K}_{3,p} = \hat{K}_{1,p} \otimes \hat{M}_{1,p} \otimes \hat{M}_{1,p} + \hat{M}_{1,p} \otimes \hat{K}_{1,p} \otimes \hat{M}_{1,p} + \hat{M}_{1,p} \otimes \hat{M}_{1,p} \otimes \hat{K}_{1,p} \tag{14}$$

with the one-dimensional mass and stiffness matrix

$$\hat{M}_{1,p} = \int_{-2}^{2} [\Phi_1]^\top [\Phi_1] \, \mathrm{d}x \quad \text{and} \quad \hat{K}_{1,p} = \int_{-2}^{2} \frac{\mathrm{d}}{\mathrm{d}x} [\Phi_1]^\top \frac{\mathrm{d}}{\mathrm{d}x} [\Phi_1] \, \mathrm{d}x, \tag{15}$$

respectively.

Concerning the basis $[\Phi_1]$, a wavelet based basis $[\Psi_p]$ has been introduced in [6, (3.46)] by the relation

$$[\Psi_p] = [\Phi_1] W_p \tag{16}$$

where $W_p \in \mathbb{R}^{2p-1 \times 2p-1}$ is the corresponding nonsingular basis transformation matrix. This basis is almost stable in $L_2(-2,2)$ and $H_0^1(-2,2)$ as the following theorem states.

Theorem 3.4 *Let $[\Psi_p]$ be defined via* (16)*. Moreover, let $\chi > 1$. Then, the relations*

$$c_{m,1}^{-1} \left(D_M \underline{u}, \underline{u}\right) \leq \| u \|_{L_2(-2,2)}^2 \leq (\log p \log^\chi \log p) c_{m,2} \left(D_M \underline{u}, \underline{u}\right), \tag{17}$$

and

$$(\log p \log^\chi \log p)^{-1} c_{k,1}^{-1} \left(D_K \underline{u}, \underline{u}\right) \leq \| u \|_{H^1(-2,2)}^2 \leq c_{k,2} \left(D_K \underline{u}, \underline{u}\right) \tag{18}$$

hold for any $u = [\Psi_p]\underline{u}$, $\underline{u} \in \mathbb{R}^{2p-1}$, where D_M and D_K are suitable chosen diagonal matrices. The constants $c_{m,1}$, $c_{k,2}$, $c_{m,2}$ and $c_{k,1}$ are independent of p. Moreover, the operations $W_p \underline{x}$ and $W_p^\top \underline{x}$ require $\mathcal{O}(p)$ floating point operations.

Proof. The constructive proof which includes also the definitions of D_M and D_K has been given in [6].

Due to (15) and (16), the relations (17) and (18) are equivalent to the spectral equivalence relations

$$c_{m,1}^{-1} D_M \leq W_p^\top \hat{M}_{1,p} W_p \leq (\log p \log^\chi \log p) c_{m,2} D_M \quad \text{and}$$
$$(\log p \log^\chi \log p)^{-1} c_{k,1}^{-1} D_K \leq W_p^\top \hat{K}_{1,p} W_p \leq c_{k,2} D_K. \tag{19}$$

Hence, we are able to introduce the preconditioner

$$\hat{C}_{3,p}^{-1} = (W_p \otimes W_p \otimes W_p) \tag{20}$$
$$(D_K \otimes D_M \otimes D_M + D_M \otimes D_K \otimes D_M + D_M \otimes D_M \otimes D_K)^{-1} (W_p \otimes W_p \otimes W_p)^\top$$

for $\hat{K}_{3,p}$ (14). Using (14), (20), (19) and the properties of the Kronecker product, we arrive at

$$\frac{1}{\log p \log^\chi \log p} \hat{C}_{3,p} \preceq \hat{K}_{3,p} \preceq (\log p \log^\chi \log p)^2 \hat{C}_{3,p} \tag{21}$$

for any $\chi > 1$.

Remark 1. The results can be extended to Neumann boundary nodes. However, a different wavelets basis, see [6, Theorem 3.9], has to be used into the space directions of one layer of elements instead of (16).

Finally, the ASM preconditioner with inexact subproblem solvers is defined as

$$C_{in,\zeta}^{-1} = P_0^\top C_{BPX}^{-1} P_0 + \sum_{\mathtt{v}} P_{\mathtt{v}}^\top \hat{C}_{3,p}^{-1} P_{\mathtt{v}}, \tag{22}$$

where C_{BPX} denotes the BPX-preconditioner, [10], and $\hat{C}_{3,p}$ is the preconditioner (20). Then, the following result is formulated.

Theorem 3.5 *Let $a(\cdot,\cdot)$ be the bilinear form* (2) *and let $C_{in,\zeta}$ be defined by* (22). *Moreover, let us assume that Assumption 3.3 is satisfied. Then, the condition number estimate $\kappa(C_{in,\zeta}^{-1} \mathscr{K}_\zeta) \preceq (\log p \log^\chi \log p)^3$ holds for any $\chi > 1$ where the constant is independent on h and p but may depend on D, c and the geometry. Moreover, the action $C_{in,\zeta}^{-1} \underline{r}$ requires $\mathscr{O}(N)$ operations.*

Proof. Due to Assumption 3.3, we have $\hat{K}_{3,p} \sim C_{\mathtt{v}}$ for all interior nodes $\mathtt{v}$, see also [19]. The result also holds for Neumann nodes with some modifications, cf. Remark 1. Using (21), Theorem 3.1 and the properties of the BPX-preconditioner, [33], the assertion follows.

3.2 The preconditioner for Lamé

In this subsection, we assume that the bilinear form $a(\cdot,\cdot)$ has the form (3) which is the bilinear form for linear elasticity. Using Korn's inequality, it can be proved, see e.g. [9], that

$$c_1 \parallel u \parallel_{H^1}^2 \leq a(u,u) \leq c_2 \parallel u \parallel_{H^1}^2 \quad \forall u \in (H_{\Gamma_1}^1(\Omega))^3. \tag{23}$$

This suggests to choose the preconditioner

$$C_{Lame,\zeta} = \begin{bmatrix} C_{in,\zeta} & \mathbf{0} & \mathbf{0} \\ \mathbf{0} & C_{in,\zeta} & \mathbf{0} \\ \mathbf{0} & \mathbf{0} & C_{in,\zeta} \end{bmatrix} \tag{24}$$

for $\mathscr{K}_\zeta$. Then, the following result can be proved.

Theorem 3.6 *Let $a(\cdot,\cdot)$ be the bilinear form* (3) *and let $C_{Lame,\zeta}$ be defined by* (24). *Moreover, let us assume that Assumption 3.3 is satisfied. Then, $\kappa(C_{Lame,\zeta}^{-1}\mathscr{K}_\zeta) \preceq (\log p \log^\chi \log p)^3$ for any $\chi > 1$ where the constant is independent on h and p but may depend on E, ν and the geometry. The action $C_{Lame,\zeta}^{-1}\underline{r}$ requires $\mathscr{O}(N)$ operations.*

Proof. The result is a direct consequence of (24), (23) and Theorem 3.5.

4 Numerical Experiments

In this section, several numerical experiments show the performance of the preconditioners (22) and (24) for scalar elliptic equations and the system of Lamé equations, respectively. The preconditioners have been implemented into the *hp*-version of the program `SPCad3H`, [7]. Several cases are considered. In each example, a coarse finite element mesh of Level 1 is read from a data file. The computational mesh is obtained by uniform refinement with respect to h and p. In all examples, the corresponding system of linear equations is solved with the pcg-method using the preconditioners (22) and (24) for scalar elliptic problems and linear elasticity, respectively. The relative accuracy of $\varepsilon = 10^{-5}$ is chosen.

4.1 Scalar elliptic problems

The first example is the Poisson equation on the unit `cube` with pure Dirichlet boundary conditions. More precisely,

- the bilinear form is chosen as (2) with $D(x) = 1$ and $c(x) = 0$,
- the right hand side is chosen randomly,
- the computational domain is $\Omega = (0,1)^3$ and $\Gamma_1 = \partial\Omega$,
- the coarse mesh consists of one element.

The iteration numbers and the computational time are displayed in Table 1. For comparison, Table 2 displays the pcg-iteration numbers and computational time with a diagonal preconditioner $\mathrm{diag}(\hat{K}_{3,p})$ instead of $\hat{C}_{3,p}$. From the results, it can be observed that the application of the preconditioner (22) reduces the iteration numbers and computational time dramatically. The numbers of iterations of the pcg-method

Levels	2		3		4		5		6	
p	It	Time[sec]	It	Time[sec]	It	Time[sec]	It	Time[sec]	It	Time[sec]
3	2	0.01	14	0.09	16	0.83	18	9.13	18	80.04
5	2	0.02	14	0.41	17	4.82	18	48.54	.	
7	11	0.06	25	1.73	25	18.18	23	148.57	.	
9	9	0.12	22	3.18	21	34.82	20	296.88	.	
11	12	0.28	29	7.51	28	79.26	.		.	
13	15	0.59	37	16.55	34	153.59	.		.	
15	16	1.02	38	25.00	35	224.81	.		.	
17	12	1.12	29	29.77	27	268.38	.		.	
19	16	2.16	.		.		.		.	
21	17	3.24	.		.		.		.	
33	15	15.53	.		.		.		.	

Table 1 Pcg-iterations on the unit `cube` with preconditioner (22).

Levels	2		3		4		5		6	
p	It	Time[sec]	It	Time[sec]	It	Time[sec]	It	Time[sec]	It	Time[sec]
3	11	0.01	64	0.23	94	2.77	96	218.41	93	174.67
5	46	0.08	229	3.16	251	27.31	250	22.08	.	
7	128	0.61	443	16.79	472	141.12	464	1115.28	.	
9	261	2.56	643	49.92	761	471.69	747	3712.70	.	
11	451	8.44	884	131.13	1084	1288.15	.		.	
13	662	21.50	1234	314.39	1293	2648.33	.		.	
15	882	49.73	1634	730.42	1685	6048.34	.		.	
17	1128	89.72	2075	1515.78	2124	10822.79	.		.	
19	1430	170.54	.		.		.		.	
21	1738	291.68	.		.		.		.	
33	4323	4084.91	.		.		.		.	

Table 2 Pcg-iterations on the unit `cube` with diagonal preconditioner.

grow moderately with respect to p. One iteration with preconditioner (22) requires about two to three times compared to a pcg-iteration of the unpreconditioned system. With an higher relative accuracy of the pcg method, similar results can be observed. For example, 85 and 130 iterations are required in order to reduce the initial error up to a factor of $\varepsilon = 10^{-10}$ and $\varepsilon = 10^{-15}$, respectively, for $p = 15$ and $Level = 3$.

Due to the Kronecker product structure, the wavelet preconditioner (20) can be made robust against anisotropies of the diffusion coefficient in (2) see [6, Remark 4.2]. However, this structure goes lost by using the preconditioner (21). In order to check this, the next example `cube.aniso` uses

- the diffusion coefficient $D(x) = \begin{bmatrix} 100 & 0 & 0 \\ 0 & 1000 & 0 \\ 0 & 0 & 1 \end{bmatrix}$.

The other parameters are chosen as in the previous example `cube`. The results are displayed in Table 3. The pcg-iteration numbers do not blow up only in Level 2 where the summation in (22) is running over one node v only, e.g. the preconditioner

p / Level	1	3	5	7	9	11	13	15	17	19	21	33
2	2	2	2	15	11	16	18	21	15	19	21	18
3	9	103	291	492	739	955	1155	1237	1297			
4	28	220	498	793	1094	1357	1667	1710	1745			
5	75	411	826	1232	1656							
6	125	663										

Table 3 Pcg-iteration numbers for `cube.aniso` with anisotropic diffusion.

is almost of the form (20). Then, the robustness of the wavelet construction can be observed. Otherwise, no robustness against anisotropies can be observed.

The next example considers the `Fichera` corner. More precisely,

- the bilinear form is chosen as (2) with $D(x) = 1$ and $c(x) = 0$,
- the right hand side is $f = 1$,
- the computational domain is $\overline{\Omega} = [-1,1]^3 \backslash (0,1]^3$ and $\Gamma_1 = \partial\Omega$,
- the coarse mesh consists of seven congruent cubes of volume 1.

Slices of the solution and the coarse mesh are displayed in Figure 3. The pcg-

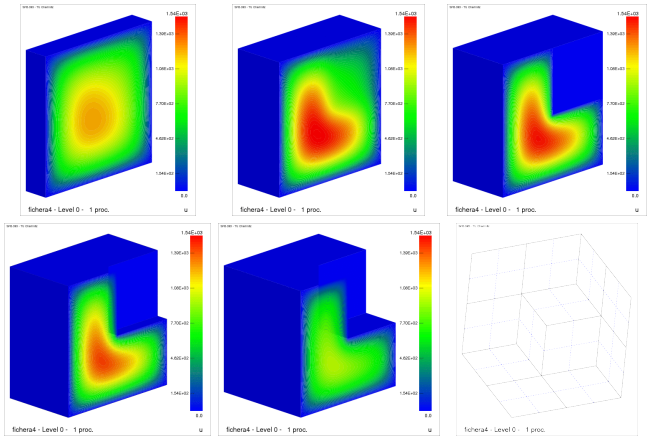

Fig. 3 Solution for the `Fichera` corner (slices at different x-values) and coarse mesh (right, below).

iteration numbers are displayed in Table 4. The behavior is similar in comparison to the unit `cube`.

The influence of coefficient `jumps` is investigated in the following coarse mesh consisting of two cubes. More precisely,

- the bilinear form is chosen as (2) with $D(x) = \begin{cases} 1 & z > 0 \\ b & z \leq 0 \end{cases}$ and $c(x) = 0$,
- the right hand side is chosen as $f(x) = \begin{cases} 1 & z > 0 \\ 0 & z \leq 0 \end{cases}$,

Level \ p	3	5	7	9	11	13	15	17	19
2	18	19	28	26	31	37	37	31	37
3	30	31	36	34	37	39	39		
4	35	35	39	37					
5	36	37							
6	31								

Table 4 Pcg-iteration numbers for the `Fichera` corner.

- the computational domain is $\Omega = (-1,1)^2 \times (-2,2)$ and $\Gamma_1 = \partial\Omega$,
- the coarse mesh consists of two congruent cubes of volume 2.

As observed in Table 5, the dependence of the jumps of the coefficients in the diffusion results in an increase of the pcg iteration numbers, in particular for higher levels of refinement.

Level \ p	3	5	7	9	11	13	15	17	19	21	33
2	6	6	16	13	18	22	23	17	23	24	22
3	17	17	26	22	29	39	40	29			
4	18	19	25	21	27	33					
5	19	19									

Level \ p	3	5	7	9	11	13	15	17	19	33
2	7	7	48	35	58	70	77	51	73	71
3	52	51	133	105	150	185	185	145		
4	63	62	113	88	126	145				
5	57	50								

Table 5 Pcg-iteration numbers for coefficient `jumps` $b = 1$ (left) and $b = 100$ (right).

4.2 Lamé equations of linear elasticity

The next examples consider the system of Lamé equations (3). More precisely,

- the bilinear form is chosen as (3) with $E = 10^6$ and $\nu = 0.3$,
- the right hand side is chosen as $f = \begin{pmatrix} 1 & 1 & 1 \end{pmatrix}^\top$,
- the computational domain is the unit `cube3.030` $\Omega = (0,1)^3$ or the domain $\overline{\Omega} = [-3,3]^3 \backslash \{(-1,1)\times(-3,3)^2 \cup (-3,3)\times(-1,1)\times(-3,3) \cup (-3,3)^2\times(-1,1)\}$ with `holes`, see Figure 4.
- all boundary conditions are chosen to be Dirichlet, e.g. $\Gamma_1 = \partial\Omega$,
- the coarse mesh consists of one element or twenty elements of volume eight, respectively.

Now, the preconditioner (24) is used. The results are displayed in Table 6. The moderate increase of iteration numbers is similar to the Poisson case. In both cases, the absolute numbers are moderately higher than for Poisson which is due to (23).

In all previous examples, the boundary conditions are of Dirichlet type. The next example investigates mixed boundary conditions for three different computational domains. In all cases, the parameters $E = 10^6$ and $\nu = 0.3$ are chosen

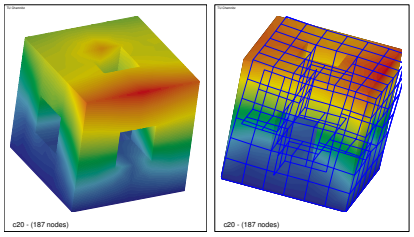

Fig. 4 Computational domain with `holes` and `holesN` (left), Displacements for `holesN` (right).

Level \ p	3	5	7	9	11	13	15	17	19	33
2	10	10	18	18	21	26	27	21	17	25
3	27	29	42	38	50	63	65	51	66	
4	28	29	41	36	47	58	60	66		
5	29	30	39							
6	30									

Level \ p	3	5	7	9	11	13	15	17	19	23
2	27	28	36	32	43	50	53	42	53	59
3	32	34	47	42	56					
4	34									

Table 6 Pcg-iteration numbers for linear elasticity, unit `cube3.030` (left), domain with `holes` (right).

as in the previous cases. No volume force exists, e.g. $f(x) = 0$. In the first case, the computational domain is a `brick` which is fixed at the bottom face, e.g. there are homogeneous Dirichlet boundary conditions. A surface force of the form $f_1(x,y,z) = \begin{pmatrix} 0 & 0 & -1 \end{pmatrix}^\top$ acts on the top face whereas no volume forces act on the other faces, e.g. $f_1(x,y,z) = 0$, see Figure 5. The coarse mesh consists of one element only. In the second case, the computational domain is a `beam` of the form $(0,2)^2 \times (0,10)$, which is fixed at the face $x = 0$. A surface force of the form $f_1(x,y,z) = \begin{pmatrix} 0 & 0 & -0.25 \end{pmatrix}^\top$, acts on the face $x = 10$, see also Figure 5. In the third case, the computational domain `holesN` is as `holes`. The domain is fixed at the bottom face $z = -3$. A surface force of the form $f_1(x,y,z) = \begin{pmatrix} 1 & 0 & -1 \end{pmatrix}^\top$, acts on the face $x = 3$, see also Figure 4. The pcg iteration numbers are displayed in Table 7. On the one hand, the absolute iteration numbers are higher than for problems with pure Dirichlet boundary conditions, cf. with the examples `cube3.030` and `holes`. On the other hand, the pcg-iteration numbers depend only moderately on the polynomial degree. Another reason for relatively high pcg iteration numbers in the example `brick` is the deformation of the elements. They are not cubes whereas the preconditioner (24) has been developed for the cubes.

Due to (23), the preconditioner (24) is not robust with respect to $\nu \to \frac{1}{2}-$ since the constant c_1 depends on ν. This is observed in the next example `cube3.049`, where a contraction ratio $\nu = 0.49$ is chosen, see Table 8. In this example, the computational domain is the unit cube. Pure Dirichlet boundary conditions are used.

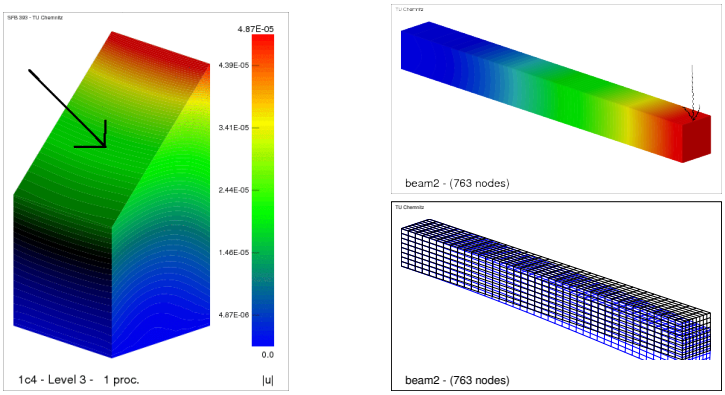

Fig. 5 Setting for the examples `brick` (left) and `beam` (right, top). The total displacement is shown colored. The displacements for `beam` are shown right, below.

Lev.	brick					beam					holesN				
p	1	3	5	7	9	1	3	5	7	9	1	3	5	7	9
2	21	70	83	91	96	68	170	183	189	189	42	71	75	76	75
3	34	83	99	106	110	117	181	193	202	201	49	72	76	78	77
4	45	89	105	113		145	188	197			56	73	76		

Table 7 Pcg-iteration numbers for mixed boundary conditions: `brick`(left), `beam` (middle) and `holesN` (right).

p	3	5	7	9	11	13	15	17	19	21	33
Level											
2	25	28	53	46	58	76	81	59	80	87	76
3	78	90	137								
4	85	90	131								
5	89										
6	90										

Table 8 Pcg-iteration numbers on the unit `cube3.049` for linear elasticity with $\nu = 0.49$.

5 Conclusion

The paper has presented a quasioptimal solver for systems of linear algebraic equations arising from the discretization of H^1 elliptic problems in three space dimensions using the hp-version of the finite element method. The efficiency of the solver has been shown in several numerical examples.

However, this solver seems not be robust against anisotropies in the coefficients, coefficient jumps or a contraction ratio ν close to 0.5. The last problem can be resolved by using a mixed formulation for linear elasticity by introducing the hydrostatic pressure p as additional variable. The mathematical details will be presented in a forthcoming paper where solvers for hp-fem discretizations of the Stokes problem are investigated.

Acknowledgement: This work has been supported by the FWF project P20121 and P23484. The basis of the code has been developed during the work at SFB 393 "Numerische Simulation an massive parallelen Rechnern". Further support has been given by the SFB F013 and the Austrian Academy of Sciences.

References

[1] M. Ainsworth. A preconditioner based on domain decomposition for h-p finite element approximation on quasi-uniform meshes. *SIAM J. Numer. Anal.*, 33(4):1358–1376, 1996.

[2] P. F. Antonietti and P. Houston. A class of domain decomposition preconditioners for hp-discontinuous Galerkin finite element methods. *J. Sci. Comput.*, 46(1):124–149, 2011.

[3] I. Babuška, A. Craig, J. Mandel, and J. Pitkäranta. Efficent preconditioning for the p-version finite element method in two dimensions. *SIAM J.Numer.Anal.*, 28(3):624–661, 1991.

[4] S. Beuchler. Multi-grid solver for the inner problem in domain decomposition methods for p-FEM. *SIAM J. Numer. Anal.*, 40(3):928–944, 2002.

[5] S. Beuchler. A domain decomposition preconditioner for p-FEM discretizations of two-dimensional elliptic problems. *Computing*, 74(4):299–317, 2005.

[6] S. Beuchler. Wavelet solvers for hp-FEM discretizations in 3D using hexahedral elements. *Comput. Methods Appl. Mech. Engrg.*, 198(13-14):1138–1148, 2009.

[7] S. Beuchler, A. Meyer, and M.Pester. SPC-PM3AdH v1.0-programmers manual. Technical Report SFB393 01-08, Technische Universität Chemnitz, March 2001.

[8] S. Beuchler, R. Schneider, and C. Schwab. Multiresolution weighted norm equivalences and applications. *Numer. Math.*, 98(1):67–97, 2004.

[9] Dietrich Braess. *Finite elements*. Cambridge University Press, Cambridge, third edition, 2007. Theory, fast solvers, and applications in elasticity theory, Translated from the German by Larry L. Schumaker.

[10] J. Bramble, J. Pasciak, and J. Xu. Parallel multilevel preconditioners. *Math. Comp.*, 55(191):1–22, 1991.

[11] Claudio Canuto, Paola Gervasio, and Alfio Quarteroni. Finite-element preconditioning of G-NI spectral methods. *SIAM J. Sci. Comput.*, 31(6):4422–4451, 2009/10.

[12] M. Costabel, M. Dauge, and L. Demkowicz. Polynomial extension operators for H^1, $H(\mathrm{curl})$ and $H(\mathrm{div})$-spaces on a cube. *Math. Comp.*, 77(264):1967–1999, 2008.

[13] L. Demkowicz. *Computing with hp Finite Elements*. CRC Press, Taylor and Francis, 2006.

[14] M. O. Deville and E. H. Mund. Finite element preconditioning for pseudospectral solutions of elliptic problems. *SIAM J. Sci. Stat. Comp.*, 18(2):311–342, 1990.

[15] B. Guo and W. Gao. Domain decomposition method for the hp-version finite element method. *Comp. Methods Appl. Mach. Eng.*, 157:524–440, 1998.

[16] B. Guo and J. Zhang. Stable and compatible polynomial extensions in three dimensions and applications to the p and h-p finite element method. *SIAM J. Numer. Anal.*, 47(2):1195–1225, 2009.

[17] G. Haase, U. Langer, and A. Meyer. Domain decomposition preconditioners with inexact subdomain solvers. Technical Report 192, TU Chemnitz, 1991.

[18] W. Hackbusch. *Multigrid Methods and Applications*. Springer-Verlag. Heidelberg, 1985.

[19] S. Jensen and V. G. Korneev. On domain decomposition preconditioning in the hierarchical $p-$version of the finite element method. *Comput. Methods. Appl. Mech. Eng.*, 150(1–4):215–238, 1997.

[20] G.M. Karniadakis and S.J.Sherwin. *Spectral/HP Element Methods for CFD*. Oxford University Press. Oxford, 1999.

[21] V. Korneev and A. Rytov. Fast domain decomposition algorithm discretizations of 3-d elliptic equations by spectral elements. *Comput. Methods Appl. Mech. Engrg.*, 197(17-18):1443–1446, 2008.

[22] V. G. Korneev. Почти оптимальныи метод решения задач Дирихле на подобластях декомпосиции иерархическои hp-версии. Дифференциальные Уравнения, 37(7):1008–1018, 2001. An almost optimal method for Dirichlet problems on decomposition subdomains of the hierarchical hp-version.

[23] J. Mandel. Iterative solvers by substructuring for the p-version finite element method. *Comput. Methods Appl. Mech. Eng.*, 80(1-3):117–128, 1990.

[24] R. Munoz-Sola. Polynomial liftings on a tetrahedron and applications to the h-p version of the finite element method in three dimensions. *SIAM J. Numer. Anal.*, 34(1):282–314, 1996.

[25] L. F. Pavarino. Additive schwarz methods for the p-version finite element method. *Numer. Math.*, 66(4):493–515, 1994.

[26] L. F. Pavarino and O. B. Widlund. Iterative substructuring methods for spectral elements in three dimensions. In *Krizek, M. (ed.) et al., Finite element methods. 50 years of the Courant element. Conference held at the Univ. of Jyväskylä, Finland, 1993. Inc. Lect. Notes Pure Appl. Math. 164, 345-355* . New York, NY: Marcel Dekker , 1994.

[27] L.F. Pavarino and O. Widlund. A polylogarithimc bound for an iterative substructuring method for spectral elements in three dimensions. *SIAM J. Numer. Anal.*, 33(4):1303–1335, 1996.

[28] J. W. Ruge and K. Stüben. *Algebraic Multigrid*, chapter 4, pages 73–130. Multigrid methods. SIAM, Philadelphia, 1987.

[29] Joachim Schöberl, Jens M. Melenk, Clemens Pechstein, and Sabine Zaglmayr. Additive Schwarz preconditioning for p-version triangular and tetrahedral finite elements. *IMA J. Numer. Anal.*, 28(1):1–24, 2008.

[30] C. Schwab. *$p-$ and $hp-$finite element methods. Theory and applications in solid and fluid mechanics.* Clarendon Press. Oxford, 1998.

[31] P. Solin, K. Segeth, and I. Dolezel. *Higher-Order Finite Element Methods*. Chapman and Hall, CRC Press, 2003.

[32] A. Toselli and O. Widlund. *Domain Decomposition Methods- Algorithms and Theory*. Springer, 2005.

[33] X. Zhang. Multilevel Schwarz methods. *Numer. Math.*, 63:521–539, 1992.